2018 European Control Conference (ECC)
June 12-15, 2018. Limassol, Cyprus

A hierarchical optimization-based scheme for combined Fire-tube Boiler/CHP generation units

Stefano Spinelli[1,2], Marcello Farina[2] and Andrea Ballarino[1]

Abstract— **In this paper we propose a hierarchical control structure to optimize the behaviour of a generation unit composed of a fire tube boiler, that supplies steam, and a combined heat and power internal combustion engine, which produces the electrical power. Simulation results are presented to show the effectiveness of the proposed scheme.**

I. INTRODUCTION

Steam plays a central role in production in many sectors. Nowadays, steam generation is often integrated with electricity production in cogenerative systems or in combined cycle plants. In many cases, these facilities are under-utilized and they are asked to respond to varying steam and electricity demand. This offers the flexibility to benefit from a greater integration with the power grid, exploiting price volatility.

In this paper we focus on a small load application composed of Fire Tube Boilers (FTB), as steam suppliers, and combined heat and power (CHP) Internal Combustion Engines (ICE) for the electrical generation. FTBs are compact systems used in small scale industries, where steam pressure and capacity are relatively limited, but demand is fluctuating. FTBs are composed of a vessel, filled up with water, where hot combustion gasses run in several submerged tubes. For cogeneration, ICEs are integrated with FTB to locally fulfil the electricity demand with on-site generation and to exploit the produced heat to enhance the efficiency of steam generation. ICE offers two useful sources of heat: i) the engine cooling circuit to pre-heat boiler feedwater and ii) exhaust gases, directed into the boiler tubes, for steam generation.

Boiler control is classically done by decoupled PID loops on water level and pressure, governed respectively by feedwater and fuel flow rates [1]. Most of the works on boiler control, [2] and references herein, focus on the drum boiler (DB), used in power plants: here water level control is a severe issue due to the shrink and swell effect. Other works, [3], [4], address FTBs, focusing on the pressure loop, as in FTBs the level control is a minor problem.

ICE control is aimed principally in maintaining the rotational speed of the motor in presence of varying load. In this work, ICE low level control systems are assumed to be in place and are not subject here of further study.

*This work was partially supported by the SYMBIOPTIMA project. SYMBIOPTIMA has received funding from the European Union's Horizon 2020 research and innovation programme, grant agreement No° 680426

[1] Istituto di Tecnologia Industriale e Automazione, Consiglio Nazionale delle Ricerche, 20133 Milan, Italy [name.surname] @itia.cnr.it

[2] Dipartimento di Elettronica, Informazione e Bioingegneria, Politecnico di Milano, 20133 Milan, Italy [name.surname] @polimi.it

Recently, research interest moved towards the integrated control of cogenerative plants, as the Boiler-Turbine (BT) unit. In [5] a MPC reference governor is proposed to control a BT unit, considering it as a unique system. Instead, the FTB and ICE systems can operate both separately and integrated: therefore, the higher level has to be able to manage this hybrid behaviour. [6] presents a similar approach for the top layer for an application on micro-grids. For the generalized Unit Commitment (UC) problem of co-generative plants, in [7] a direct MILP formulation is used, while in [8] an hybrid system approach is presented.

In this paper, we propose a hierarchical control structure to optimize the behaviour of a Generation Unit (GU) composed of the integrated FTB/ICE CHP and to dynamically control the internal variables of the systems. The higher level (HL) addresses the operational optimization and the UC problem of the co-generation in a scenario with price fluctuations and varying demands by solving an hybrid optimization problem, while the lower level (LL) Model Predictive Controller (MPC), receiving the operation point from the HL, guarantees that the process constraints of the individual systems are fulfilled. The paper is structured as follows: Section II presents the subsystem models used at high and low hierarchical levels, Section III describes in detail the proposed control structure. Section IV describes the simulation results of the application of the proposed control scheme to the generation unit. Finally, in Section V some conclusions are given.

II. MODELS

A. The CHP Dynamic Model in full operation mode

The small-scale Internal Combustion Engine CHP is a natural gas engine linked to a 3-phase synchronous generator. ICE exhaust gases can be diverted through a valve in a set of tubes of the fire tube boiler, to reduce the overall request of natural gas of the integrated systems. In full operation mode, it is modelled as lumped system: a mean value engine model connected with a static generator, based on [9]. The states of the system are the angular speed ω of the motor and the engine internal pressure p^{CHP}, while the inputs are the gas mass flow rate $q^{\mathrm{CHP}}_{\mathrm{GAS}}$ and the electrical demand $P^{\mathrm{CHP}}_{\mathrm{El}}$. The exhaust gas enthalpy, $H^{\mathrm{CHP}}_{\mathrm{ex}}$, depends of the state of the system. The parameters of the dynamic model are derived from the physical and geometric properties of the considered CHP. Also, a fine tuning of the gain matrix has been carried out based on the available static data: for confidentiality reasons, data are not shown. However, for completeness, Fig. 1 shows a comparison between the static map obtained

with available data and the one computed using the identified model.

In this paper, we control the angular speed ω to the nominal value $\bar{\omega} = 50Hz$ using a standard PI controller acting on the input $q_{\rm GAS}^{\rm CHP}$. The control law has been tuned in such a way that the settling time is smaller than 1 s. In this way, the so-obtained closed-loop system is characterized by one input only, i.e., the electrical demand $P_{\rm El}^{\rm CHP}$, while the gas flow rate $q_{\rm GAS}^{\rm CHP}$ and the exhaust gas enthalpy $H_{\rm ex}^{\rm CHP}$ are to be considered as system outputs. Importantly, the state of the system has an assessment time of about 0.5 s, while the sampling time of the "fast" MPC controller, that will be designed at the low hierarchical level in Section III-B, is $\tau_{\rm L} = 60$ s. In such a timescale one can assume the CHP to be in steady-state conditions, with the static gain sufficient to represent the CHP behaviour and with the power produced by the CHP equal to $P_{\rm El}^{\rm CHP}$.

The variable $q_{\rm GAS}^{\rm CHP}$, in full operation mode, is constrained to lie in a set, where also a lower bound is defined.

$$q_{\rm GAS}^{\rm CHP} \in [q_{\rm min}^{\rm CHP}, q_{\rm max}^{\rm CHP}] \tag{1}$$

where $q_{\rm max}^{\rm CHP} > q_{\rm min}^{\rm CHP} > 0$.

B. The CHP High-Level Hybrid Automaton

The model for the HL optimizer, sampling time $\tau_{\rm H} = 15$ min, must comprise the steady-state behaviour of the CHP in all its operation modes and therefore a discrete hybrid automaton (DHA) [10] is used, including both discrete and continuous states.

The discrete state $m^{\rm CHP}$ corresponds with the CHP operation mode, i.e., shut down (OFF), cold start (CS), hot start (HS), and production (ON). The dynamic state is denoted with $\tau^{\rm CHP}$, i.e. the time spent in the present operation mode. The output of the model, $(q_{\rm GAS}^{\rm CHP}, H_{\rm ex}^{\rm CHP})$, depends upon both the operation mode $m^{\rm CHP}$ and the produced electric power $P_{\rm El}^{\rm CHP}$. In the mode $m^{\rm CHP} = {\rm ON}$, the CHP behaviour is represented by the static gain between its input, $P_{\rm El}^{\rm CHP}$, and its output pair $(q_{\rm GAS}^{\rm CHP}, H_{\rm ex}^{\rm CHP})$. For simplicity, affine relationships are identified with available data, i.e.

$$\begin{array}{rcl} q_{\rm GAS}^{\rm CHP} & = & (P_{\rm El}^{\rm CHP} - P_{\rm int})/\gamma_q \\ H_{\rm ex}^{\rm CHP} & = & \gamma_h P_{\rm El}^{\rm CHP} \end{array} \tag{2a}$$

where $P_{\rm int}$, γ_q, and γ_h are identified from data, as shown in Fig. 1. In all other operating modes, $(P_{\rm El}^{\rm CHP}, H_{\rm ex}^{\rm CHP})$ are null,

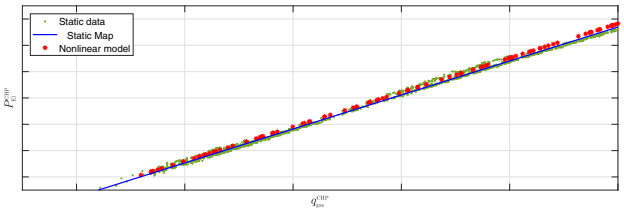

Fig. 1. Relationship between $q_{\rm GAS}^{\rm CHP}$ and $P_{\rm El}^{\rm CHP}$ in steady-state conditions. Green dots: experimental data; red dots: static map of the nonlinear model devised in Section II-A; blue line: identified affine relationship (2a). (x and y axes are adimensional).

while the gas is consumed both in CS and HS modes. More specifically

$$(q_{\rm GAS}^{\rm CHP}, H_{\rm ex}^{\rm CHP}) = \begin{cases} (0,0) & \text{if } m^{\rm CHP} = {\rm OFF} \\ (q_{\rm CS}^{\rm CHP}, 0) & \text{if } m^{\rm CHP} = {\rm CS} \\ (q_{\rm HS}^{\rm CHP}, 0) & \text{if } m^{\rm CHP} = {\rm HS} \end{cases} \tag{2b}$$

In (2b), $q_{\rm CS}^{\rm CHP}$ and $q_{\rm HS}^{\rm CHP}$ are the required flow rates in the cold start and hot start, respectively, phases.

Transitions, as depicted in Fig. 2, are possible only if the time

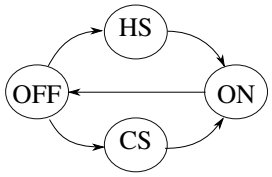

Fig. 2. Possible transitions between operation modes of the CHP.

spent in the current operating mode $\tau^{\rm CHP}(k)$ is greater than a proper threshold. Also, the ON $\rightarrow$ OFF transition and the starting ones (OFF $\rightarrow$ CS and OFF $\rightarrow$ HS) are triggered when a proper switching input signal $u_{\rm S}^{\rm CHP}(k) \in \{0,1\}$ is set to 1. So, at each time step k, invariance conditions are:

$$\begin{array}{rcl} [{\rm OFF}] \wedge ([\tau^{\rm CHP}({\rm k}) \leq \tau_{\rm OFF\rightarrow HS}] \vee [\neg {\rm u}_{\rm S}^{\rm CHP}({\rm k})]) & \Longrightarrow & [{\rm OFF}] \\ [{\rm CS}] \wedge [\tau^{\rm CHP}({\rm k}) \leq \tau_{\rm CS\rightarrow ON}] & \Longrightarrow & [{\rm CS}] \\ [{\rm HS}] \wedge [\tau^{\rm CHP}({\rm k}) \leq \tau_{\rm HS\rightarrow ON}] & \Longrightarrow & [{\rm HS}] \\ [{\rm ON}] \wedge ([\tau^{\rm CHP}({\rm k}) \leq \tau_{\rm ON\rightarrow OFF}] \vee [\neg {\rm u}_{\rm S}^{\rm CHP}({\rm k})]) & \Longrightarrow & [{\rm ON}] \end{array}$$

with $\tau^{\rm CHP}(k+1) = \tau^{\rm CHP}(k) + 1$.

The transition conditions are:

$$\begin{array}{rcl} [{\rm OFF}] \wedge [\tau^{\rm CHP}({\rm k}) \geq \tau_{\rm OFF\rightarrow CS}] \wedge [{\rm u}_{\rm S}^{\rm CHP}({\rm k})] & \Longrightarrow & [{\rm CS}] \\ [{\rm OFF}] \wedge [\tau_{\rm OFF\rightarrow HS} \leq \tau^{\rm CHP}({\rm k}) \leq \tau_{\rm OFF\rightarrow CS}] & & \\ \wedge [u_{\rm S}^{\rm CHP}(k)] & \Longrightarrow & [{\rm HS}] \\ [{\rm CS}] \wedge [\tau^{\rm CHP}({\rm k}) \geq \tau_{\rm CS\rightarrow ON}] & \Longrightarrow & [{\rm ON}] \\ [{\rm HS}] \wedge [\tau^{\rm CHP}({\rm k}) \geq \tau_{\rm HS\rightarrow ON}] & \Longrightarrow & [{\rm ON}] \\ [{\rm ON}] \wedge [\tau^{\rm CHP}({\rm k}) \geq \tau_{\rm ON\rightarrow OFF}] \wedge [{\rm u}_{\rm S}^{\rm CHP}({\rm k})] & \Longrightarrow & [{\rm OFF}] \end{array}$$

with reset condition $\tau^{\rm CHP}(k+1) = 0$.

The values of $\tau_{\rm OFF\rightarrow HS}$, $\tau_{\rm OFF\rightarrow CS}$, $\tau_{\rm CS\rightarrow ON}$, $\tau_{\rm HS\rightarrow ON}$, and $\tau_{\rm ON\rightarrow OFF}$, are suitably-defined thresholds.

C. The Boiler dynamic model in full operation mode

The mathematical model of the fire tube boiler in full operation mode is inspired by [11]. Differently from [11] we have two sources of heat, i.e., the gas burner and the exhaust gases diverted from the CHP. The set of equations describing the system dynamics is

$$\begin{array}{rcl} \dfrac{d}{dt}[\rho_{\rm s} V_{\rm s} + \rho_{\rm w} V_{\rm w}] & = & q_{\rm f} - q_{\rm s} \\ \dfrac{d}{dt}[\rho_{\rm s} e_{\rm s} V_{\rm s} + \rho_{\rm w} e_{\rm w} V_{\rm w}] & = & Q_{\rm m\rightarrow w}^{\rm t,GAS} + Q_{\rm m\rightarrow w}^{\rm t,CHP} + q_{\rm f} h_{\rm f} - q_{\rm s} h_{\rm s} \\ \dfrac{d}{dt}[m^{\rm t,GAS} C_p T^{\rm t,GAS}] & = & Q_{\rm GAS}^{\rm B} - Q_{\rm m\rightarrow w}^{\rm t,GAS} \\ \dfrac{d}{dt}[m^{\rm t,CHP} C_p T^{\rm t,CHP}] & = & \alpha_{ex} \eta_{\rm ex} H_{\rm ex}^{\rm CHP} - Q_{\rm m\rightarrow w}^{\rm t,CHP} \end{array} \tag{3}$$

where ρ, V, q, T, h, and e denote the density, volume, mass flow rate, temperature, and specific enthalpy and energy, respectively of steam (s), water (w), and feedwater (f). $m^{\mathrm{t,GAS}}$ (respectively, $m^{\mathrm{t,CHP}}$) denotes the mass of the tubes heated by the gas burner (respectively, transporting exhaust gases from the CHP), while $T^{\mathrm{t,GAS}}$ (respectively, $T^{\mathrm{t,CHP}}$) denotes its temperature and C_p is the heat capacity. Also, $\alpha_{\mathrm{ex}} \in \{0,1\}$ is the status of the diverting valve (open/closed), and η_{ex} denotes the rate of enthalpy of the exhaust gases that can be transmitted to the tubes. Since the system works at saturated conditions, the water and steam pressures satisfy the equality $p_{\mathrm{w}} = p_{\mathrm{s}} = p(T_{\mathrm{w}})$. Also,

$$Q^{\mathrm{B}}_{\mathrm{GAS}} = \eta C_{\mathrm{LHV}} q^{\mathrm{B}}_{\mathrm{GAS}}$$

where C_{LHV} is the lower heating value and $q^{\mathrm{B}}_{\mathrm{GAS}}$ is the combustion gas flow rate. The heat transmitted from the metal walls to the water can be modelled as

$$Q^{\mathrm{t,GAS}}_{\mathrm{m}\to\mathrm{w}} = \xi(T^{\mathrm{t,GAS}} - T_{\mathrm{w}})$$
$$Q^{\mathrm{t,CHP}}_{\mathrm{m}\to\mathrm{w}} = \xi(T^{\mathrm{t,CHP}} - T_{\mathrm{w}})$$

where ξ is the heat transfer coefficient, based on Cooper correlation, depending on the boiling two phase mixture of steam and water close to the tube walls.

The model parameters have been analytically computed based on the physical and geometric properties of the system. A fine tuning has been conducted on available data. The manipulable inputs are the feedwater, q_{f}, and the combustible gas flow rates, $q^{\mathrm{B}}_{\mathrm{GAS}}$. The steam flow rate q_{s}, the exhaust gas opening level α_{ex}, and the exhaust gas enthalpy $H^{\mathrm{CHP}}_{\mathrm{ex}}$ are to be considered, in the low-level control, as exogenous disturbances. The output variables that will be controlled at the low hierarchical level are the steam pressure p_{s} and the water level inside the boiler, l_{w}. The inputs and outputs are subject to constraints:

$$q_{\mathrm{f}} \in [0, q_{\mathrm{f,max}}] \tag{4a}$$
$$q^{\mathrm{B}}_{\mathrm{GAS}} \in [q^{\mathrm{B}}_{\mathrm{min}}, q^{\mathrm{B}}_{\mathrm{max}}] \tag{4b}$$
$$p_{\mathrm{s}} \in [p_{\mathrm{min}}, p_{\mathrm{max}}] \tag{4c}$$
$$l_{\mathrm{w}} \in [l_{\mathrm{min}}, l_{\mathrm{max}}] \tag{4d}$$

D. The Boiler High-Level Hybrid Automaton

The boiler model for the HL optimizer must comprise the steady-state behaviour of the FTB in all its operation modes. Similarly to the CHP model, a DHA [10] is devised.

Since two discrete values are possible for the exhaust valve opening (open/closed), two different production modes are introduced. In this way, the discrete state m^{B} takes values in the set $\{\mathrm{OFF}, \mathrm{CS}, \mathrm{HS}, \mathrm{ON}_{\alpha=0}, \mathrm{ON}_{\alpha=1}\}$.

The model, in operation modes $\mathrm{ON}_{\alpha=0}$ and $\mathrm{ON}_{\alpha=1}$, is assumed to be in steady-state conditions and under control, in such a way that $p_{\mathrm{s}} = \bar{p}_{\mathrm{s}}$ and $l_{\mathrm{w}} = \bar{l}_{\mathrm{w}}$, where $\bar{p}_{\mathrm{s}}$ and $\bar{l}_{\mathrm{w}}$ are suitable and fixed nominal conditions. In this way, the combustion gas flowrate required to fulfill the steam request $q^{\mathrm{B}}_{\mathrm{GAS}}$ results to be a function of q_{s} and, in case $\alpha_{\mathrm{ex}} = 1$, also of $H^{\mathrm{CHP}}_{\mathrm{ex}}$. For simplicity, an affine relationship is identified

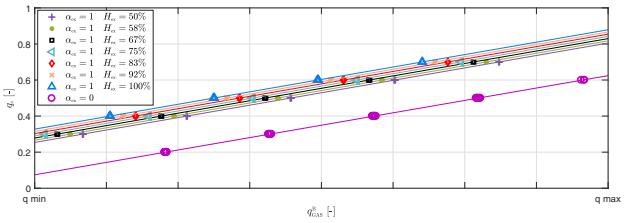

Fig. 3. Relationship between $q^{\mathrm{B}}_{\mathrm{GAS}}$ and q_{s} in steady-state conditions. The identified static map (5) is presented for different values of $\alpha_{\mathrm{ex}} H_{\mathrm{ex}}$ in solid lines. Markers show the steady-state data of the nonlinear model (3).

and used by the high level control layer:

$$q^{\mathrm{B}}_{\mathrm{GAS}} = \alpha_1 q_{\mathrm{s}} + \alpha_2 \alpha_{\mathrm{ex}} H^{\mathrm{CHP}}_{\mathrm{ex}} + \alpha_3 \tag{5}$$

where α_1, α_2, and α_3 are identified from the model static map, as shown in Fig. 3. In all the other modes of operation, the produced steam flow rate is null, while the gas flow rate is present both in CS and HS modes, similarly to equation (2b). Also in case of the FTB, transitions are possible only if the time spent in the current operating mode τ^{B} is greater than a proper threshold. Also, both the switch-off and switch-on transitions are triggered when a proper switching input signal $u^{\mathrm{B}}_{\mathrm{S}}(k) \in \{0,1\}$ is set to 1. Further details are omitted for sake of brevity.

III. Hierarchical Control Structure

The utility demand and the price forecast are given and known for a 24 hours horizon. The surplus of electricity can be sold to the power grid, and, if negative, it can be bought from the grid. The proposed hierarchical control structure includes a high optimization layer that aims to optimize the performance of the integrated plant on a day-ahead basis with a sampling time of $\tau_{\mathrm{H}} = 15$ min. The block scheme of the model used at high level is sketched in Fig. 4. The high

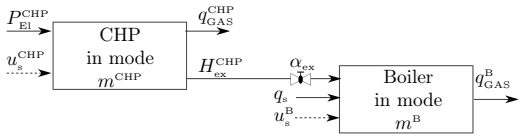

Fig. 4. Sketch of the high-level model.

level optimizer receives as input the 24-hours ahead electric and steam demands $P^{\mathrm{D}}_{\mathrm{El}}(k)$ and $q^{\mathrm{D}}_{\mathrm{s}}(k)$, respectively, for $k = 1, \ldots, 96$, together with a forecast of the electricity prices. Based on this, the optimizer determines the future modes of operation of the systems $m^{\mathrm{CHP}}(k)$ and $m^{\mathrm{B}}(k)$, as well as the optimal production profiles $P^{\mathrm{CHP}}_{\mathrm{El}}(k)$, $q_{\mathrm{s}}(k)$ and the corresponding predicted combustion gas amounts $q^{\mathrm{CHP}}_{\mathrm{GAS}}(k)$ and $q^{\mathrm{B}}_{\mathrm{GAS}}(k)$ for the whole future optimization time horizon. The lower level is faster, with a sampling time of $\tau_{\mathrm{L}} = 60$ s, aiming to control the dynamic variables of the subsystems. For clarity, the symbol h denotes the discrete time index in the fast time scale of the lower layer, while k the time index in the slow high-level time scale.

A. The high level optimization problem

The objective of the HL optimizer is to minimize, at a day-ahead basis, the operating costs of the plant with the constraint of a complete fulfilment of the electric and steam demands in a liberalized energy market. A further degree of freedom for the optimization is introduced by the possibility either to buy/sell electricity $P_{\mathrm{El}}^{\mathrm{Purch}}$ from/to the power grid, to complement the ICE production. The ICE and the FTB are to be considered in an integrated fashion because of the valve present to divert exhaust gases from the CHP to a set of tubes in the boiler. It can be opened only when the engine is in production, i.e. $\alpha_{\mathrm{ex}} = 1 \implies m^{\mathrm{CHP}} = \mathrm{ON}$. To formulate the HL optimization problem, the two DHAs devised in Sections II-B and II-D are integrated in a single Mixed Logical Dynamical (MLD) system [12] of the type:

$$\begin{aligned} x_{\mathrm{H}}^{+} &= A_{\mathrm{H}} x_{\mathrm{H}} + B_{\mathrm{H},1} u_{\mathrm{H}} + B_{\mathrm{H},2} \Delta_{\mathrm{H}} + B_{\mathrm{H},3} z_{\mathrm{H}} \\ y_{\mathrm{H}} &= C_{\mathrm{H}} x_{\mathrm{H}} + D_{\mathrm{H},1} u_{\mathrm{H}} D_{\mathrm{H},2} \Delta_{\mathrm{H}} + D_{\mathrm{H},3} z_{\mathrm{H}} \\ E_{\mathrm{H},4} \Delta_{\mathrm{H}} &+ E_{\mathrm{H},5} z_{\mathrm{H}} \leq E_{\mathrm{H},1} u_{\mathrm{H}} + E_{\mathrm{H},4} x_{\mathrm{H}} + E_{\mathrm{H},5} \end{aligned} \tag{6}$$

where the state, $x_{\mathrm{H}} = [\tau^{\mathrm{CHP}}, x_b^{\mathrm{CHP}}, \tau^{\mathrm{B}}, x_b^{\mathrm{B}}]^{\mathrm{T}}$, is composed of real and boolean variables and x_{H}^{+} is the state at the next step $(k+1)$. The input of the MLD system $u_{\mathrm{H}} = [u_{\mathrm{S}}^{\mathrm{CHP}}, q_{\mathrm{GAS}}^{\mathrm{CHP}}, u_{\mathrm{S}}^{\mathrm{B}}, q_{\mathrm{GAS}}^{\mathrm{B}}, \alpha_{\mathrm{ex}}, P_{\mathrm{El}}^{\mathrm{Purch}}]^{\mathrm{T}}$ is composed of, respectively, the switching signals and the natural gas mass flow rates of the ICE and FTB subsystems, the divert valve command and the electricity purchased from the grid. The output is $y_{\mathrm{H}} = [P_{\mathrm{El}}, q_{\mathrm{S}}^{\mathrm{B}}]^{\mathrm{T}}$, where $P_{\mathrm{El}} = P_{\mathrm{El}}^{\mathrm{CHP}} + P_{\mathrm{El}}^{\mathrm{Purch}}$ is the electric power both purchased and generated by the ICE and the latter is the steam produced by the boiler. Δ_{H} and z_{H} are, respectively, auxiliary binary and continuous variables. Last equation in (6) includes both the inequalities related to the logical relationships that regulate the switches between discrete states, and the operational constraints (1) and (4). The cost function is given by:

$$J_{\mathrm{H}} = C_{fuel} - R \tag{7}$$

where the fuel cost C_{fuel} is related to fuel consumption used to respect the utility demand as follows:

$$C_{fuel} = \sum_{k} (q_{\mathrm{GAS}}^{\mathrm{CHP}}(k) + q_{\mathrm{GAS}}^{\mathrm{B}}(k)) \lambda_{gas} \tag{8}$$

The cost (8) considers also the costs related to the start up modes $\{\mathrm{CS}, \mathrm{HS}\}$, due to the gas flow values defined in (2b) also for the non productive phases. The revenue term R in (7) is related to the possibility of selling the electricity surplus to the grid. It can take into account also the purchase of electricity, in case $R < 0$. By splitting the deviation from the electrical demand in positive and negative fluctuation, $\Delta^{\uparrow} e$, $\Delta^{\downarrow} e$, it is possible to consider different prices for electricity, i.e., whether it is sold or bought:

$$R = \sum_{k} \Delta^{\uparrow} e(k) \lambda_{\uparrow}(k) - \Delta^{\downarrow} e(k) \lambda_{\downarrow}(k) \tag{9}$$

with

$$\begin{aligned} &\Delta e(k) = P_{\mathrm{El}}^{\mathrm{CHP}}(k) + P_{\mathrm{El}}^{\mathrm{Purch}}(k) - P_{\mathrm{El}}^{\mathrm{D}}(k) \\ &\Delta e(k) = \Delta^{\uparrow} e(k) - \Delta^{\downarrow} e(k) \\ &\Delta^{\uparrow} e(k), \Delta^{\downarrow} e(k) \geq 0 \quad \forall k \end{aligned}$$

The optimization problem can be stated as follows, where the initial time is $k = 1$ for simplicity reasons:

$$\begin{aligned} \min_{\zeta(1) \ldots \zeta(N_{\mathrm{H}})} \quad & J_{\mathrm{H}} \\ \text{s.t.} \quad & \text{MLD model (6)} \\ & P_{\mathrm{El}}^{\mathrm{CHP}}(k) + P_{\mathrm{El}}^{\mathrm{Purch}}(k) \geq P_{\mathrm{El}}^{\mathrm{D}}(k) \\ & q_{\mathrm{S}}^{\mathrm{B}}(k) \geq q_{\mathrm{S}}^{\mathrm{D}}(k) \\ & P_{\mathrm{El}}^{\mathrm{Purch}}(k) \geq 0 \\ & \text{for all } k = 0, ..., N_{\mathrm{H}} \end{aligned}$$

where $\zeta(k) = [u_{\mathrm{H}}(k), \Delta_{\mathrm{H}}(k), z_{\mathrm{H}}(k)]'$ and $N_{\mathrm{H}} = 96$ are the intervals in the horizon and $q_{\mathrm{S}}^{\mathrm{D}}$ is the steam demand. The HL optimization generates the profiles of binary and continuous inputs that minimize the economic cost function of the GU for the given utility demand.

B. The low level control

The CHP control is not a practical issue, as it has to just operate at a fixed rotational speed $\bar{\omega} = 50Hz$ and physical constraints are not imposed: as discussed in Section II, a standard PI controller is in place. Conversely, the LL control of the FTB is critical. In particular, we consider the control problem of the boiler in full operation modes $\mathrm{ON}_{\alpha=0}$ and $\mathrm{ON}_{\alpha=1}$, while the proposal of innovative control strategies for the remaining modes of operation will be subject of future work. As described in Section II, the boiler must satisfy input and output constraints to operate safely: the water level l_{w} and the steam pressure p_{s} must be maintained in the bounded ranges (4d) and (4c). Violating the lower bound in (4d) exposes the boiler tubes outside the water, while, if the upper bound is violated, water or wet steam may enter the distribution network. Pressure constraints are defined based on the range acceptable by the steam consumers: as the system operates at saturation, constraints can be converted to water temperature constraints.

The low-level controller will be committed to enforce these limitations while steering the boiler outputs to the nominal setpoints. This controller requires a linear discrete-time model of the boiler, which is obtained from (3). For simplicity, in this paper only one fixed nominal linearization point has been selected. We define the state, input, and output vectors of the state-space model as $x_{\mathrm{L}} = [T^{\mathrm{t,GAS}}, T^{\mathrm{t,CHP}}, l_{\mathrm{w}}, T_{\mathrm{w}}]^{\mathrm{T}}$, $u_{\mathrm{L}} = [q_{\mathrm{f}}, q_{\mathrm{GAS}}^{\mathrm{B}}]^{\mathrm{T}}$, and $y_{\mathrm{L}} = [l_{\mathrm{w}}, T_{\mathrm{w}}]^{\mathrm{T}}$. Also, the model is characterized by the presence of two types of measured disturbances, i.e. the steam flow rate q_{s} and the term $\alpha_{\mathrm{ex}} H_{\mathrm{ex}}^{\mathrm{CHP}}$: while the latter is not manipulable (since $H_{\mathrm{ex}}^{\mathrm{CHP}}$ is an output of the CHP and the state of α_{ex} is

selected by the high level optimizer), the former is indeed manipulable, although a gas flow request $q_{\mathrm{s}}^{\mathrm{D}}$ is assumed to be given, to be fulfilled at any time instant. However, this request may not be feasible in some cases, e.g., in transient conditions and with real demand different from the forecast used for scheduling at the high level. So, it is beneficial for the low-level control to use q_{s} as a further degree of freedom, to be set equal to the demanded $q_{\mathrm{s}}^{\mathrm{D}}$ if possible.

The linearization point is characterized by the values $x_{\mathrm{L}}^{\mathrm{ss}}$, $u_{\mathrm{L}}^{\mathrm{ss}}$, $y_{\mathrm{L}}^{\mathrm{ss}}$, $q_{\mathrm{s}}^{\mathrm{ss}}$, and $H_{\mathrm{ex}}^{\mathrm{CHP,ss}}$, while the vectors of the corresponding linearized system

$$\delta x_{\mathrm{L}}^{+} = A_{\mathrm{L}}\delta x_{\mathrm{L}} + B_{\mathrm{L,u}}\delta u_{\mathrm{L}} + B_{\mathrm{L,q}}\delta q_{\mathrm{s}} + B_{\mathrm{L,ex}}\delta v_{\mathrm{ex}}$$
$$\delta y_{\mathrm{L}} = C_{\mathrm{L}}\delta x_{\mathrm{L}} + D_{\mathrm{L,u}}\delta u_{\mathrm{L}} + D_{\mathrm{L,q}}\delta q_{\mathrm{s}} + D_{\mathrm{L,ex}}\delta v_{\mathrm{ex}}$$

are defined as $\delta x_{\mathrm{L}} = x_{\mathrm{L}} - x_{\mathrm{L}}^{\mathrm{ss}}$, $\delta u_{\mathrm{L}} = u_{\mathrm{L}} - u_{\mathrm{L}}^{\mathrm{ss}}$, $\delta y_{\mathrm{L}} = y_{\mathrm{L}} - y_{\mathrm{L}}^{\mathrm{ss}}$, $\delta q_{\mathrm{s}} = q_{\mathrm{s}} - q_{\mathrm{s}}^{\mathrm{ss}}$, $\delta v_{\mathrm{ex}} = \alpha_{\mathrm{ex}} H_{\mathrm{ex}}^{\mathrm{CHP}} - H_{\mathrm{ex}}^{\mathrm{CHP,ss}}$ and $\delta x_{\mathrm{L}}^{+} = \delta x_{\mathrm{L}}(h+1)$.

The aim of the controller is, if possible, to fulfill the steam demand ($\delta_{\mathrm{s}}^{D} = q_{\mathrm{s}}^{D} - q_{\mathrm{s}}^{\mathrm{ss}}$), while regulating the output δy_{L} to the nominal operating condition $(0, 0)$. The input setpoint is defined as $\delta u_{\mathrm{L}}^{\mathrm{opt}} = u_{\mathrm{L}}^{\mathrm{ref}} - u_{\mathrm{L}}^{\mathrm{ss}}$, where $u_{\mathrm{L}}^{\mathrm{ref}}$ is defined based on $q_{\mathrm{s}}^{D}(h)$ and $H_{\mathrm{ex}}^{\mathrm{CHP}}(h)$ using a steady-state maps, e.g. (5).

The MPC defines the input by solving the following quadratic programming problem, at each time step h:

$$\min_{\delta u_{\mathrm{L}}(h),\ldots,\delta u_{\mathrm{L}}(h+p),\delta q_{\mathrm{s}}(h),\ldots,\delta q_{\mathrm{s}}(h+p)} \quad J_{\mathrm{L}} \tag{10}$$

$$\begin{aligned} \text{s.t.} \quad \delta q_{\mathrm{f}} &\in [0 - q_{\mathrm{f}}^{\mathrm{ss}}, q_{\mathrm{f,max}} - q_{\mathrm{f}}^{\mathrm{ss}}] \\ \delta q_{\mathrm{GAS}}^{\mathrm{B}} &\in [q_{\mathrm{min}}^{\mathrm{B}} - q_{\mathrm{GAS}}^{\mathrm{B,ss}}, q_{\mathrm{max}}^{\mathrm{B}} - q_{\mathrm{GAS}}^{\mathrm{B,ss}}] \\ \delta T_{\mathrm{w}} &\in [T_{\mathrm{min}} - T_{\mathrm{w}}^{\mathrm{ss}}, T_{\mathrm{max}} - T_{\mathrm{w}}^{\mathrm{ss}}] \\ \delta l_{\mathrm{w}} &\in [l_{\mathrm{min}} - l_{\mathrm{w}}^{\mathrm{ss}}, l_{\mathrm{max}} - l_{\mathrm{w}}^{\mathrm{ss}}] \end{aligned}$$

where $J_{\mathrm{L}} = \sum_{j=h}^{h+p} \|\delta y_{\mathrm{L}}(j)\|_{Q}^{2} + \|\delta u_{\mathrm{L}}(j) - \delta u_{\mathrm{L}}^{\mathrm{opt}}(j)\|_{R}^{2} + \|\delta q_{\mathrm{s}}(j) - \delta q_{\mathrm{s}}^{\mathrm{D}}(j)\|_{Q_{\mathrm{s}}}^{2}$ and where the used notation is consistent with the previous definitions. A slack variable can be introduced to further enforce the feasibility of the optimization problem at all time instants. The matrices Q, R, Q_{s} are properly-defined positive-definite matrices; note that, in order to give priority to the fulfilment of the steam demand, we can set $Q_{\mathrm{s}} >> \lambda_{\max}(Q), \lambda_{\max}(R)$.

At time instant h, the optimal values $\delta u_{\mathrm{L}}(h|h)$ and $\delta q_{\mathrm{s}}(h|h)$ are obtained: therefore, the input $u_{\mathrm{L}}(h) = u_{\mathrm{L}}^{\mathrm{ss}} + \delta u_{\mathrm{L}}(h|h)$ is applied to the real system and the steam flow rate $q_{\mathrm{s}}(h) = q_{\mathrm{s}}^{\mathrm{ss}} + \delta q_{\mathrm{s}}(h|h)$ is actually provided.

If the steam demand $q_{\mathrm{s}}^{D}(h)$ and/or the real CHP exhaust flow rate profile $H_{\mathrm{ex}}^{\mathrm{CHP}}(h)$ differ from the values considered at the high scheduling level, the steady-state points reached by the controlled system will possibly differ from the ones selected by the high level optimizer. This, however, is not critical since the major goal of the controller is to guarantee that the operational constraints are enforced at all time instants.

If, in any case, the real values of $q_{\mathrm{s}}^{D}(h)$ and/or $H_{\mathrm{ex}}^{\mathrm{CHP}}(h)$ differ dramatically from the scheduled ones, the high level optimizer may be required to be run again (with new and more reliable scheduled steam and electric power demands) in order to recompute, for the following time steps, more realistic optimal setpoints.

IV. Simulation Results

We validate the proposed hierarchical optimization approach through simulation, using the nonlinear models of the GU presented in Section II. The FTB is a 3-pass 10 bar steam generator with nominal steam flowrate $\bar{q}_s = 1200$ kg/h and the CHP is a 12-valve natural gas ICE producing up to $\bar{P}_{\mathrm{El}}^{\mathrm{CHP}} = 1200$ kW. The FTB and the ICE must provide the demanded steam and electrical power, satisfying the permitted ranges: $q_{\mathrm{GAS}}^{\mathrm{Boiler}} \in [12.5\%, 100\%]$, $q_{\mathrm{f}}^{\mathrm{Boiler}} \in [0, 0.35]$ kg/h, $p_{\mathrm{s}} \in [9.5, 10.5]$ bar, $l_{\mathrm{w}} \in [0.95, 1.05]\bar{l}_{\mathrm{w}}$ and $P_{\mathrm{El}}^{\mathrm{CHP}} \in [50\%, 100\%]$.

The MLD model (6) is implemented using the hybrid system description language (HYSDEL) [13].

The electricity price is supposed to vary on hourly basis, see

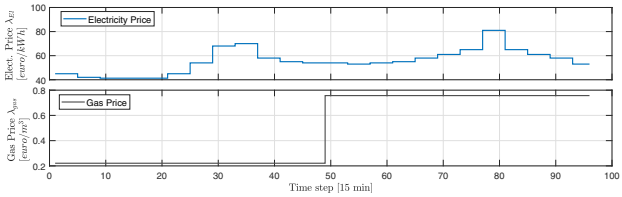

Fig. 5. Electricity price (top). Gas price (bottom). At $k = 48$ gas price is increased to show by simulation the effect of relative electricity/gas price on the GU behaviour.

Fig. 5, and its values are taken from the historical database of day-ahead market of *Gestore Mercati Energetici* (GME). For the purpose of highlighting the effect of a different utility price ratio and to show this in a unique graph, the price of natural gas is artificially increased at time $k = 48$. A random realization of the fluctuating profiles of electricity and steam demands of the consumers is generated for the simulation. For the higher layer, mode transition times are the following: $\tau_{\mathrm{OFF}} = (1; 1)$, $\tau_{\mathrm{OFF}\to\mathrm{CS}} = (5; 3)$, $\tau_{\mathrm{CS}\to\mathrm{ON}} = (4; 2)$, $\tau_{\mathrm{HS}\to\mathrm{ON}} = (1; 1)$ and $\tau_{\mathrm{ON}} = (3; 3)$, respectively for the FTB and the ICE.

Fig. 6 shows the results of the HL optimization. The first and the third panels from the top describe the evolution of the operative modes of CHP and FTB, respectively, while the other two panels show the demanded and produced electricity and steam, respectively. The electricity supply is split between the contribution of CHP generation (in dotted blue line) and electricity purchased from the grid (solid magenta). The gas/electricity price ratio affects the optimal strategy of the GU: for $k < 48$, where grid electricity is relatively more expensive, the CHP fulfils the electrical demand alone and, whenever it is convenient, it sells the electricity surplus. In the opposite case, for $k \geq 48$, the CHP is maintained in minimum production mode, just to take advantage of the diverted gas into the FTB for steam production, while the remaining electricity demand is covered purchasing power from the grid. However, in high steam demand points, i.e., for $k = [73, 83)$, the effect of full power ICE is beneficial both in terms of electricity surplus and boiler efficiency. The reference trajectory computed by the optimization layer is provided to the LL-MPC controller described in Section III-B, which operates when the FTB is in production modes.

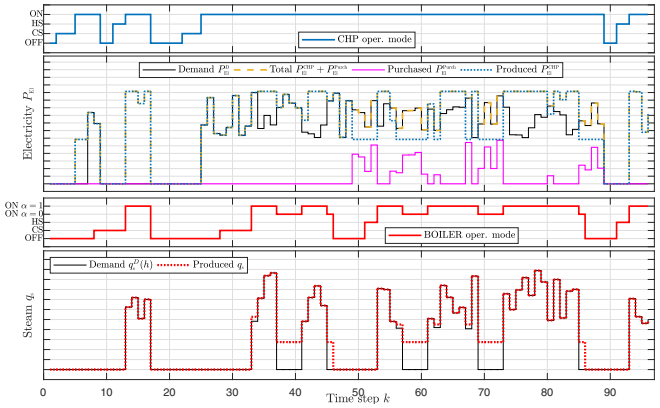

Fig. 6. Simulation results of HL optimization: at $\tau = 48$ the gas price is switched to high. i) CHP operating modes. ii) Electricity demand and supply. iii) FTB operating modes. iv) Steam demand and production.

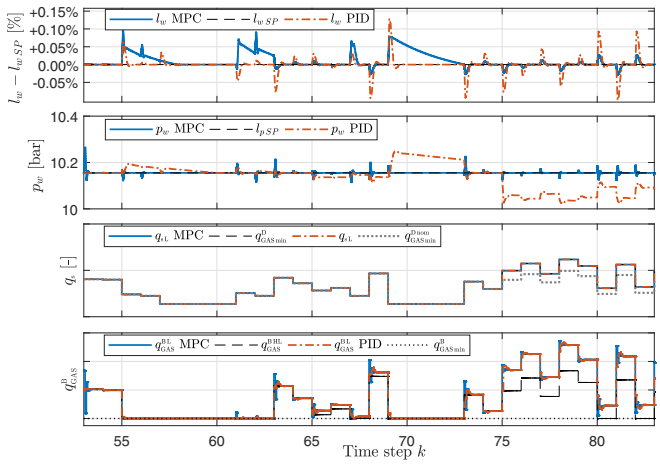

Fig. 7. LL MPC (solid) and PID (dash-dot) controllers. i) Water level. ii) Steam pressure. iii) Produced steam flow rate. iv) Boiler gas flow rate. *Nominal*: $k = [53, 65) \cup [72, 75)$; *Scenario a*: $H_{ex} = 0.75\, H_{ex\,HL}$, in $k = [65, 72)$; *Scenario b*: $k = [75, 83]$, $q_{\rm s} = 1.25\, q_{\rm s\,HL}$.

The linear model is computed around a single nominal operating point of $q_{s\,0} = 0.5\bar{q}_s$ and $H_{\rm ex\,0}^{\rm CHP} = 0.5\bar{H}_{\rm ex}^{\rm CHP}$. The MPC regulates the $\delta q_{\rm GAS}^{\rm B}$ and $\delta q_{\rm f}$ to maintain the steam pressure and the water level close to their set points and inside the valid ranges. To highlight the advantages of a MIMO optimal controller at low level, in Fig. 7 we show a comparison with a classic PID control scheme, based on two separate control loops for level and pressure regulation. PIDs have been tuned at our best to be effective in the nominal operating point. To show the robustness properties of the hierarchical control approach here presented, in the simulation we assume that the demand used for computing the low-level input setpoints (equal to the one assumed by the high level optimizer) is different in term of electricity (*Scenario a*) or steam (*Scenario b*) with respect to the real request. The two different scenarios are presented in the same graph, along with the nominal case.

- *Nominal*: $k = [53, 65) \cup [72, 75)$, the LL regulates the FTB along the trajectory defined by the HL. Different control behaviours when actuator saturation occurs: MPC can be easily tuned to give priority to the pressure control.

- *Scenario a*: electricity produced is decreased by 25% with respect to the HL assumption in $k = [65, 72)$. A lower contribution of H_{ex} is provided to the boiler: both PID and MPC controllers increase the $\delta q_{\rm GAS}^{\rm B}$ to fill the gap of exhaust gasses. However, PID stabilizes on a lower pressure level.

- *Scenario b*: steam demand $q_{\rm s\,HL}$ is artificially increased by 25% for $k = [75, 83)$: the implemented PID controller cannot regulate correctly the pressure, while maintains the level to the desired set-point.

V. Conclusions

In this paper we have proposed a hierarchical control structure to optimize the behaviour of a generation unit composed of a fire tube boiler and a combined heat and power internal combustion engine. Simulation results are presented to show the effectiveness of the proposed scheme. Future work will address a number of issues. For example, the dynamic control and optimization of the boiler start-up phases will be investigated. Also, we will consider, in the future, the optimization of a number of similar generation units: this will possibly pave the way to tailored distributed optimization and control schemes.

References

[1] Dukelow, S.G., Liptk, B.G., Cheng, X. and Meeker, R.H., (2013). Boiler Control and Optimization. In Liptk, Process Control: Instrument Engineers' Handbook, Elsevier Science, pp. 1572-1631

[2] Lu, C.X., Rees, N.W. and Donaldson, S.C., (2005). The use of the Åström-Bell model for the design of drum level controllers in power plant boilers. IFAC Proceedings Volumes, Elsevier, 38(1), pp. 139–144

[3] Feliu-Batlle, V., Rivas Perez, R., Castillo Garcia, F., and Sotomayor Moriano, J. (2005). Fire tube industrial boilers. Fractional control. Automatica and Instrumentation, 365, pp. 90-95.

[4] Rodriguez-Vasquez, J. R., Perez, R. R., Moriano, J. S., and Gonzlez, J. P. (2008). Advanced control system of the steam pressure in a fire-tube boiler. IFAC Proceedings Volumes, 41(2), pp. 11028-11033.

[5] Klaučo, M., and Kvasnica, M. (2017). Control of a boiler-turbine unit using MPC-based reference governors. Applied Thermal Engineering, 110, pp. 1437-1447.

[6] Raimondi Cominesi, S., Farina, M., Giulioni, L., Picasso, B., and Scattolini, R. (2017). A Two-Layer Stochastic Model Predictive Control Scheme for Microgrids. IEEE Transactions on Control Systems Technology.

[7] Mitra, S., Sun, L., and Grossmann, I. E. (2013). Optimal scheduling of industrial combined heat and power plants under time-sensitive electricity prices. Energy, 54, pp. 194-211.

[8] Ferrari-Trecate, G., Gallestey, E., Letizia, P., Spedicato, M., Morari, M., and Antoine, M. (2004). Modeling and control of co-generation power plants: a hybrid system approach. IEEE Transactions on Control Systems Technology, 12(5), pp. 694-705.

[9] L. Guzzella and C. H. Onder,(2004). Introduction to Modeling and Control of Internal Combustion Engine Systems. Springer

[10] Lygeros, J., Tomlin, C., and Sastry, S. (2008). Hybrid Systems: Modeling, Analysis and Control.

[11] Ortiz, F. G. (2011). Modeling of fire-tube boilers. Applied Thermal Engineering, 31(16), pp. 3463-3478.

[12] Bemporad, A., and Morari, M. (1999). Control of systems integrating logic, dynamics, and constraints. Automatica, 35(3), pp. 407-427.

[13] Torrisi, F. D., and Bemporad, A. (2004). HYSDEL - a tool for generating computational hybrid models for analysis and synthesis problems. IEEE transactions on control systems technology, 12(2), pp. 235-249.